IGM83-181-079
CNRC 21359

FATIGUE CRACK GROWTH PREDICTION METHODS FOR VARIABLE AMPLITUDE LOADING: A REVIEW

F.G. Hamel and J. Masounave
National Research Council Canada
Industrial Material Research Institute
75, de Mortagne
Boucherville, Québec, Canada J4B 6Y4

The local strain approach for the prediction of the fatigue initation life cannot be easily used for fatigue propagation since complicating factors such as the crack closure effect arise.

Methods developed for propagation can be classified into three categories: 1) single parameter or ΔK_{eq} methods such as ΔK_{RMS}, 2) crack closure based methods and, 3) cycle-by-cycle empirical models.

Models representative of each category will be described, discussed and compared.

When overload effects are non-negligeable and when cycle-by-cycle models have to be used the empirical methods are presently preferred to those based on stronger theoretical background. However, promising studies have recently been carried out on the latter methods.

REVUE DES METHODES DE PREDICTION DE LA VITESSE DE FISSURATION EN FATIGUE SOUS CHARGEMENT D'AMPLITUDE VARIABLE

par François G. Hamel et J. Masounave
Conseil national de recherches du Canada
Institut de génie des matériaux
75 boul. de Mortagne
Boucherville, Québec, Canada J4B 6Y4

La méthode de prédiction utilisée pour l'initiation et qui porte le nom d'approche de la déformation locale ("local strain approach") peut difficilement être appliquée pour la propagation à cause de certaines particularités comme le phénomène de talonnement des lèvres de la fissures.

Les méthodes développées pour la propagation peuvent être divisées en trois catégories soit, 1) les méthodes à paramètre unique ou ΔK_{eq} telles que ΔK_{RMS}, 2) les méthodes basées sur le phénomène de fermeture ou ΔK_{eff} et enfin, 3) les méthodes faisant appel à des modèles empiriques cycle par cycle. Des modèles représentatifs de chacune des catégories sont décrits en détail, discutés et comparés entre eux.

Dans le cas où les effets de surcharges sont non négligeables et où des modèles cycle par cycle doivent être utilisés, les modèles empiriques sont plus largement utilisés que ceux appuyés sur des bases théoriques plus solides. Par contre, les travaux sur ces derniers semblent prometteurs.

INTRODUCTION

Considerable data on fatigue properties of materials under constant amplitude loading is available in the literature under the forms representative of the different aspects of the fatigue phenomenon. To employ these data, the design engineer must adapt it to the particular service conditions that he is concerned with.

The well-known stress vs life or S-N curve largely relates to the fatigue initiation behaviour of materials and defines the endurance limit which is used for design. The strain-life ($\Delta\varepsilon$-N) curve is of more recent origin and relates the elastic and plastic strain amplitudes to the initiation life.

Fatique propagation data are presented on a crack growth rate vs stress intensity factor range diagram (log da/dn vs logΔK). This curve can be divided into three portions:

1. a threshold under which there is no propagation,
2. a central region which is linear in log-log coordinates and obeys the Paris law (1),
3. a region of accelerated growth of higher slope close to the critical stress intensity factor.

Constant amplitude loading tests are generally not representative of service loading but are convenient because they are much easier to perform than variable amplitude tests and are of more general application for material characterization. On the other hand, variable amplitude tests are specific to the loading history employed and cannot be directly used for a different loading history. Consequently, there is a need for a prediction method permitting to calculate the variable amplitude fatigue behaviour of materials from constant amplitude test results. The simplest damage acculumation procedure is to assume that each single segment in a multi-level or variable amplitude loading history will produce the same damage as in constant amplitude loading. This is known as the linear damage accumulation or Palmgren-Miner's rule (2,3).

This rule neglects the interaction effects between the different loading levels. In propagation, it is a well-known fact that positive overloads will slow or even stop the crack growth rate and that a negative overload will cancel the effect of a previous overload or temporarily accelerate the crack growth rate (see for example review papers (4-6)).

When the interaction effects between levels are expected to be important, adequate prediction methods have to be used. The purpose of the present paper is to review and discuss the different methods for prediction of the crack growth rate under variable amplitude loading. However, it is useful to discuss first the case of crack initiation for which a practical and effective method exists for prediction under variable amplitude loading.

THE LOCAL STRAIN APPROACH FOR INITIATION

Examination of the stress-strain signal of a smooth specimen under variable amplitude loading (Fig. 1) will reveal the formation of closed hysteresis loops of different sizes. It has been demonstrated that the life of the sample could be adquately correlated with the total strain amplitude of the closed hysteresis loops (7-8).

A counting method known as the rainflow counting method (9) has been developped to identify the closed hysteresis loops. It is out of the scope of the present paper to describe in details the rainflow counting method, which is done elsewhere (7-8). It can be mentioned that in this method, the smaller cycles are considered as interruptions of the larger ones and the larger excursions of the loading history are paired together to define the larger cycles. The final result of the algorithm will identify each closed hysteresis loop of figure 1 as a loading cycle.

The relationship between the total strain amplitudes of the rainflow counted cycles and the life is unique for each material and the so-called strain-life curve (Fig. 2) is simply the sum of two straight lines (on a log-log plot) corresponding to the plastic and elastic strains components. In some situations when the effect of mean stress is expected to be important, a

cycle-by-cycle approach has to be used to compute the mean stress of each individual strain cycle.

For notched specimens, it has been postulated that the material at the root of the notch could be considered to behave like small cylindrical samples submitted to the same stress-strain history. The stress-strain history of the material at the root of the notch is calculated from the load history, the stress-strain properties of the material and the Neuber's rule (10,11). Then the calculation proceeds as for the smooth specimen.

This method known as the local strain approach has been shown to adequately predict the initiation time of cracks from deep notches under variable amplitude loading (7,8,11,12). The method has been developped and described in such a way that it can be applied in a straightforward manner to be used as a practical engineering design tool.

THE PROCESSES AT THE TIP OF THE PROPAGATING CRACK

A propagating fatigue crack can be considered as a very acute notch periodically reinitiating at every cycle. Since it has been possible with the local strain approach to adquately describe the intitiation of cracks from deep notches it should be possible to use the same approach for propagation, after evaluation of the local strain at the tip of the propagating crack. It is however much more difficult to measure and evaluate the stress-strain history at the tip of a fatigue crack than at the end of a deep notch.

At the tip of a fatigue crack the radius of curvature is theoretically zero producing a 1/r singularity and a very large strain gradient. The stress concentration factor concept cannot be applied and is replaced by the stress intensity factor concept. Practically, the crack tip radius is larger than zero and is not constant but is a function of the instantaneous applied load, the previous loading history and the material behaviour. The situation is complicated by an additional phenomenon not present for initiation from deep notches: the crack closure.

The crack closure was first identified by Elber (13,14) and used to explain the effect of the load ratio, R, under constant amplitude loading. The closure phenomenon can be explained by the residual compressive stresses left in the wake of the propagating crack on the sides of the fracture surface (14) and also by the plastic zone in front of the crack tip. The plastically deformed material surrounding the crack is acting as a clamp preventing the crack to open at low tensile load and reducing the effective stress intensity factor range, ΔK_{eff}. The phenomenon can be used to explain, at least qualitatively the effect of an overload on the crack growth rate.

During the overload, a large propagation increment will occur. Immediately following the overload, the crack may propagate more or less easily (depending on the material strain hardening behaviour) in the highly strained and damaged material. As the crack will penetrate into the plastic zone produced by the overload, the clamping effect caused by the compressive residual stresses will increase and will reduce the effective stress intensity factor, ΔK_{eff} and accordingly the crack growth rate. The retardation will exist as long as the crack tip remains inside the plastic zone produced by the overload. This described behaviour (instant acceleration, delayed retardation and progressive return to the original crack growth rate) have been experimentally observed. The plasticity induced closure is then considered to be responsible at least partly for the overload and underload effects observed during propagation under variable amplitude loading.

Due to closure effects and the other mentioned factors, the stress-strain history at the tip of fatigue cracks is difficult to model. Some attemps (15-19) have been done to do so and to correlate the crack growth rate to the local strain and the low cycle fatigue properties. These methods are still in the development stage especially as applied to variable amplitude loading (19). Much development must still be done for this approach to become a practical engineering tool but it is promising.

The methods which have been effectively used to predict crack growth rates under variable amplitude can be divided into three groups: 1) the single parameter or equivalent ΔK methods, 2) the crack closure based or effective

ΔK methods and 3) the cycle-by-cycle empirical models. Each of these will be explained and discussed in the following sections.

SINGLE PARAMETER OR ΔK_{eq} METHODS

The simplest method to predict the crack growth rate under variable amplitude is to replace the stress intensity factor range, ΔK, in the Paris relationship

$$\frac{da}{dN} = C\Delta K^m \qquad (1)$$

or in another appropriate da/dN vs ΔK equation by an equivalent ΔK, ΔK_{eq}, that has the same value as the constant amplitude ΔK for the same growth rate.

Barsom (20-21) proposed the root mean square of the stress intensity factor ranges, ΔK_{RMS}, as an appropriate candidate for ΔK_{eq}:

$$\Delta K_{eq} = \Delta K_{RMS} = \alpha\sigma_{RMS}(\pi a)^{\frac{1}{2}} \qquad (2)$$

where α is a geometry correction factor and

where $\sigma_{RMS} = \left[\int_0^\infty \Delta\sigma^2 \, P\,(\Delta\sigma)\, d\sigma\right]^{\frac{1}{2}}$

where $P(\Delta\sigma)$ is the density probability distribution function of the stress ranges. For its tests, Barsom used short blocks (500 cycles) with a Rayleigh function for $P(\sigma)$ and a constant σ_{min} value. For blocks of this length, the stress intensity opening load, K_{op}, is known to remain constant (14) and for a Rayleigh distribution overload effects are expected to be small; consequently, it is not possible to extrapolate the Barsom's results to different loading histories. Sullivan and Crooker (22) obtained similar results with much shorter blocks.

A sightly different ΔK_{RMS} concept was employed by Hudson (23):

$$\Delta K_{eq} = \Delta K_{RMS} = K_{maxRMS} - K_{minRMS} \tag{4}$$

where $$K_{maxRMS} = \left[\frac{1}{M} \sum_{i=1}^{M} (K_{max\ i})^2\right]^{\frac{1}{2}} \tag{5}$$

$$K_{minRMS} = \left[\frac{1}{M} \sum_{i=1}^{M} (K_{min\ i})^2\right]^{\frac{1}{2}} \tag{6}$$

This approach has the advantage that the load ratio can be defined in a manner similar to the constant amplitude case:

$$R_{RMS} = \frac{K_{minRMS}}{K_{maxRMS}} \tag{7}$$

This enables Hudson to use Forman's law (24) to account for the load ratio in his crack growth rate prediction:

$$\frac{da}{dN} = \frac{C(\ K_{RMS})^m}{(1-R_{RMS})\ K_{Ic} - K_{RMS}} \tag{8}$$

where C and m are the constant amplitude coefficients and K_{Ic} the plane-strain fracture toughness.

Hudson's work was part of an ASTM round-robin investigation (25) using a fighter aircraft loading history and its predictions, if slightly non-conservative, were competitive, due to its simplicity, with much more complex methods. However, he himself, stated that this method can only be applied to stationary random loading and not to complex histories with large non-frequent overloads for which order effects become important.

Careful inspection of Hudson's formula reveals that changing the mean value of a signal will not only change the calculated K_{RMS} but also the calculated ΔK_{RMS} which is in disagreement with the usual definition of ΔK_{RMS}. Moreover, according to equations 5 and 6, a negative peak overload will have the same contribution in the summation as a positive peak overload of the same magnitude which is in disagreement with the general experimental results. There is no theoretical argument for using the RMS value as an equivalent parameter but if it is postulated that each range in a variable amplitude loading produces the same crack increment as under constant amplitude, it can be written, as proposed by Paris (26):

$$\Delta K_{eq} = \Delta K_{RMN} = \left[\frac{1}{k} \sum_{i=1}^{k} \Delta K_i^{\,n} \right]^{1/n} \qquad (10)$$

where n is the Paris law component. This is simply a linear damage rule for propagation. Albrecht and Yamada (27) used this law for ferritic steels where n=3 and called ΔK_{RMN} the root mean cube range denoted as ΔK_{RMC}. Hibberd and Dover (28-30) used a similar law with n=2 for a low alloy NiCr steel of HY100 type and with n=3.3 for mild steel (BS4360 50C) employed in offshore structures. They obtained excellent correlation between constant and variable amplitude tests and concluded that the ΔK_{RMN} parameter, (which they referred to as the weighted average range) was superior than the ΔK_{RMS} parameter.

Kitagawa et al. (31) also used a similar approach for a cold-rolled steel with n=4. Since they were testing at very low stress levels, close to the constant amplitude threshold for propagation, ΔK_{th}, they considered in their summation that the ΔK ranges under ΔK_{th} did not contribute to propagation. Considering the results of Koterazawa et al. (32) which demonstrate that, in a variable amplitude history, the ranges under ΔK_{th} also contribute to propagation, the assumption of Kitagawa et al. might be expected to

underestimate the calculated damage. This might explain their faster crack propagation rates under variable amplitude compared to those for constant amplitude for equal ΔK_{eq} values. Their method seems to underestimate the variable amplitude ΔK_{eq} parameter, which confirms the Koterazawa et al. findings.

It is to be noted that the K_i ranges used in equation 10 are the actual consecutive ranges of the loading history. Considering the success obtained with the rainflow counting method for the prediction of fatigue initiation, an improvement of equation 10 might be to use the rainflow counted ranges for K_i.

Other authors (31,33-36) used the "true" rms value of the signal amplitude, defined as

$$\Delta K_{eq} = K_{rms} = \alpha \sigma_{rms} (\pi a)^{\frac{1}{2}} \tag{11}$$

where $$\sigma_{rms} = \left[\lim_{T \to \infty} \frac{1}{T} \int_{t}^{t+T} (\sigma - \sigma_o)^2 \, dt \right]^{\frac{1}{2}} \tag{12}$$

where σ_o is the mean value and σ the instantaneous value of the signal. This "true" rms is noted here with lower case characters as opposed to the RMS of the ranges noted with upper case characters. The two should not be confused.

Hibberd and Dover (28,30) point out that, in a non-corrosive environment, the crack growth rate ar ordinary temperatures is only a function of the signal amplitude and not of its shape. Since K_{rms} is a function of the signal shape, ΔK_{RMS} which is only a function of the ranges seems to be a more appropriate parameter. Moreover, ΔK_{RMS} and ΔK are equal for a constant amplitude sinusoidal signal but $K_{rms} = 2\sqrt{2}\Delta K$.

On the other hand, the use of σ_{rms} offers some advantages for investigators using analog techniques to generate or analyse their signals. For example, the rms value of signals produced with such techniques can be easily measured

or calculated from the power spectral density (PSD):

$$\sigma_{rms} = \left[\int_0^\infty G(f)df \right]^{\frac{1}{2}} \qquad (13)$$

where G(f) is the power spectral density function of the signal.

The power spectral density function fully describes the characteristics of a stationary random process. It can be used not only to evaluate the rms value but also the number of peaks, N_1, the number of positive mean crossings, N_o, the irregularity factor, $I=N_o/N_1$, the cumulative frequency distribution of level crossings, and the density distribution of the peaks (37-39). The irregularity factor, I, of a signal is directly related to the bandwidth of G(f): narrow-band signals have irregularity factors close to unity and inversely, wide-band signals have low irregularity factors (Fig.3).

Since two signals with the same rms value do not have the same rainflow count if they do not have the same irregularity factor, the rms alone does not fully characterize the fatigue damage. To overcome this difficulty, Wirshing and Light (40) computed a correction factor, λ, which can be used to estimate the damage produced by a wide-band random loading from the damage produced by an equivalent narrow-band random loading having the same rms and expected number of positive mean crossings, N_o. They postulated that a linear summation of the damage due to the rainflow counted ranges would provide an acccurate estimate of the damage and computed λ from simulated loading signals of different irregularity factors for different values of the slope of the S-N curve. Their results are also very useful to compute the rainflow damage for propagation under random loading of signals produced by analog techniques if the Paris law exponent is used in lieu of the S-N curve slope.

When slightly modified for the case of propagation, the equations of Wirsching and Light become:

$$\frac{da}{dn} = \lambda C \left(2 \sqrt{2} K_{rms}\right)^m \Gamma(m/2+1) \qquad (14)$$

where C and m are the Paris law coefficient and exponent,
Γ is the gamma function and,

$$\Gamma(m,\varepsilon) = a(m) + \left[1-a(m)\right] \cdot (1-\varepsilon)^{b(m)} \tag{15}$$

where $$a(m) = .926 - .033m \tag{16}$$

$$b(m) = 1.587 - 2.323m \tag{17}$$

$$\varepsilon = \sqrt{1-I_o^2} \tag{18}$$

and n, the number of cycles is based on the number of positive mean crossings, N_o.

All the previously mentioned approches use only one or two parameters to characterize the whole spectrum and cannot take into account interaction effects between the cycles. They, however, provide adequate predictions for short blocks or stationary random loadings for which overload and underload effects are negligible.

CRACK CLOSURE BASED MODELS, ΔK_{eff}

As mentioned earlier, the crack closure phenomenon has a great influence on the crack growth rate under variable amplitude loading. Prediction models based on the calculation of the effective stress intensity factor,

$$\Delta K_{eff} = K_{max} - K_{op},$$

where K_{op} corresponds to the K value at which the crack tip becomes open, have been used by many authors.

For short loading blocks of less than a few hundred cycles, Elber (41) observed that the opening stress intensity factor , K_{op}, measured with a COD gauge remains essentially constant. He proposed that for such loadings, the crack increment, δ_a, could be simply calculated from a summation of the individual crack increments for each cycle:

$$\Sigma(\delta_a)_i = A\,\Sigma(\Delta K_{eff})_i^n \qquad (19)$$

The purpose of this study however was not to develop a prediction model but only to replace a variable amplitude loading by an equivalent constant amplitude loading to reduce testing time. He did not develop a method to predict K_{op} which has to be measured experimentally for each spectrum and material.

Socie (42) used a method based on the finite element technique and the cyclic stress-strain curve of the material to calculate the opening load, S_{op}. He used the strain-life curve of the material and a rainflow count of the portion of the strain cycles over the opening point to predict the crack propagation life. His work was applied to three loading histories used for a round-robin test of the Society of Automotive Engineers (43). He obtained excellent predictions for the bracket and the transmission histories but slightly over-conservative for the suspension history which is mostly in compression. It is believed that for these relatively short histories (1708 to 5936 ranges) the opening load is essentially constant as for the Elber's work (41).

Newman's approach (44,45) is based on the Dugdale model (46) modified to account for three-dimensional effects and for the plastically deformed material left along the crack surfaces as the crack advances. The plastically deformed material is represented by perfectly plastic bar elements (Fig. 4). The model is used to calculate the displacements of the crack faces and to obtain K_{op} and consequently ΔK_{eff} for variable amplitude loading. Newman obtained good predictions for the aeronautical loadings submitted to the participants of the ASTM round-robin survey previously mentioned (25). The model correctly predicts the effects of simple and multiple overloads and underloads but involves complex numerical calculations and a cycle-by-cycle iteration scheme.

De Koning (47) developed a simpler cycle by cycle model based on the crack closure to predict crack growth rate. This model assumes that each overload leaves a hump on the crack faces. The crack is closed when the humps come in contact and opens when the humps break contact. The size of the humps depends on the magnitude of the overload and the humps can be flattened by underloads. However, some experimental data of S_{op} vs $S_{max,o}$ and S_{UL} are needed for the application of the model. The symbol $S_{max,o}$ refers to the maximum load of the overload and S_{UL} to the minimum value of the load history following the overload. Consequently, even if based on the crack closure concept, De Koning's model should be considered as semi-empirical. Although the model does not take multiple overloads into account it is much simpler to use than the Newman's model since it uses only explicit equations and not numerical approximations based on multiple bar elements. De Koning obtained excellent predictions for aeronautical loading similar to TWIST (48) consisting of 30000 cycles grouped into 2500 flights.

Sunder (49) developed a cycle-by-cycle model taking into account the instant acceleration caused by an overload and the delayed retardation. The model makes use of many empirical constants which reduces the applicability of the model. In the model, the opening load S_{op} is represented by the sum of two quantities S_{op}^{max} and S_{op}^{min} which are respectively the contribution of the preceding large overload and the minimum load of the previous cycle. For short periodic histories, S_{op}^{max} is considered constant which simplifies the model and the equations for the effective stress range (50):

$$\Delta S_{eff} = \frac{1}{n} \left[\sum_{i=1}^{n} \left[S_{max\ i} - \max \left(S_{min\ i}, S_{op}^{max} + S_{op}^{min}{}_{i} \right) \right]^{m} \right]^{1/m} \qquad (20)$$

$$\text{where } S_{op}^{min} = S_{min}\left[k_1 - k_2\,(1-R)\right] \qquad (21)$$

$$S_{op}^{max} + A S_{max}^{b} S_{RMS}^{c}$$

where m is the Paris law exponent, A, b and c are constants empirically determined for each material, S_{RMS} is the RMS of the stress ranges, and k_1 and k_2 are the coefficients of an equation proposed by Elber (14):

$$\frac{\Delta K_{eff}}{\Delta K} = U = k_1 + k_2 R \qquad (22)$$

The summation of equation 20 is performed for a single block and does not need a continuous cycle-by-cycle integration of the crack growth increments, δ_a, as for the previous methods (41,42,44,45,47). Sunder's model provided excellent prediction for aeronautical loading with and without GAG (ground-air-ground) cycles, although it was slightly overly optimistic at long lives.

Other crack closure based models (51-54) which are not sumarized here have been proposed. The studies mentioned and many others (55-57) clearly demonstrate that the crack closure effect is responsible for most of the effects observed during crack propagation tests under variable amplitude loading. On the other hand, some studies (5, 58-61) have shown that crack closure alone was not able to explain all the effects and, for instance, did not correctly predict the magnitude of the crack growth rate reduction following an overload. Models incorporating phenomena such as crack tip blunting (15,16,62-64) and the plasticity induced residual stresses (15,42,64,65) were then proposed.

These models, for example that of McCartney (64), are complex and imply laborious calculations. Moreover they often make use of adjustable empirical parameters based on experimental test results. Such approaches based on strong theoretical background are useful for the comprehension of the involved mechanism but are not practical for predicting the crack growth rate of a given material submitted to a given spectrum. For this purpose, purely empirical models based on overload test data are more widely used.

CYCLE-BY-CYCLE EMPIRICAL MODELS

The best known of the cycle-by-cycle models are those of Willenborg et al. (66) and Weeler (67). These two models are based on the same general principles illustrated in Figure 5:

1) A large overload produces a plastic zone of size r_{po};

2) Subsequent cycles are affected (produce a smaller crack increment) as long as their plastic zone, r_{pi}, remains inside that produced by the overload;

3) When a subsequent cycle produces a plastic zone large enough to extend past the overload plastic zone, this new plastic zone becomes the new overload plastic zone, r_{op}, and so on.

Wheeler (67) introduced a delay parameter, θ,

$$\frac{da}{dn} = \theta f(\Delta K) \tag{23}$$

with

$$\theta = \left[\frac{r_{pi}}{\lambda}\right]^m \tag{24}$$

where $f(\Delta K)$ is a constant amplitude crack growth law, m is an adjustable empirical material constant and $\lambda = a_o + r_{po} - a_i$ is the distance between the extension of the plastic zone due to the overload and the actual length of the crack, a_i. When $r_{pi} > \lambda$, there is no retardation and a new overload is defined as explained previously. For short periodical loadings for which $a_o = a_i$, Broek and Smith (68) proposed a semi-linear simplified version of the Wheeler model:

$$\left[\frac{da}{dn}\right]_{\text{retarded}} = \left[\frac{\sigma_{RMS}}{\sigma_{max}}\right]^m \times \left[\frac{da}{dN}\right]_{\text{linear}} \tag{25}$$

In other words, $(\sigma_{RMS}/\sigma_{max})^m$ becomes the delay parameter, θ, in this simplified model.

The model of Willenborg et al. (66) is also based on the relative dimensions of the current cyclic plastic zone and the overload plastic zone. They propose that a fictitious residual stress exists at the crack tip. This residual stress is equal to the difference between the maximum stress of the current cycle, $S_{max,i}$ and the stress required to produce a plastic zone large enough to reach the overload plastic zone limit:

$$S_{res} = S_{max\ req} - S_{max,i} \tag{26}$$

and that $S_{max\ req}$ can be expressed in terms of a stress intensity factor:

$$K_{max\ req} = \alpha S_{max\ req} \sqrt{\pi a_i} \tag{27}$$

and related to the size of the plastic zone associated with it:

$$r_{req} = a_o + r_{po} - a_i = \left[\frac{1}{2\pi} \quad \frac{K^2_{max\ req}}{\sigma^2_{ys}}\right] \tag{28}$$

where r_{req} is identical to λ in the Wheeler model, σ_{ys} is the yield strength and,

$$r_{po} = \frac{1}{2\pi} \left[\frac{K_{max,o}}{\sigma_{ys}}\right]^2 \tag{29}$$

The effective stress intensity factor, $K_{max\ eff}$, as reduced by S_{res}, becomes:

$$K_{max\ eff} = K_{max,i} - \alpha \sqrt{\pi a_i}\ S_{res} \tag{30}$$

where α, equal to α in eq. 27 is the usual geometry correction factor for stress intensity formulas. Combined with equations 26-29, equation 30 becomes:

$$K_{max\ eff} = K_{max,i} - \left[K_{max,o} \sqrt{1 - \left[\frac{a_i - a_o}{r_{po}}\right]} \quad - K_{max,i}\right] \tag{31}$$

Since S_{res}, also reduces $K_{min,i}$,

$$K_{min\ eff} = K_{min,i} - \left[K_{max,o}\sqrt{1-\left[\frac{a_i - a_o}{r_{po}}\right]} - K_{max,i}\right] \qquad (32)$$

It follows that $\Delta K_{eff} = K_{max\ eff} - K_{min\ eff}$ is not affected by an overload which only reduces the stress ratio R_{eff}. The crack increment for each cycle can be predicted from a propagation law which takes the stress ratio, R, into account, for example, Forman's law (24) (eq.8).

As pointed out by Broek (69), equation 26 which implies that the residual stress is a function of the maximum stress of the current cycle, $S_{max,i}$, can be considered as questionable. These empirical models, however, do not have to be based on a strong theoretical background but should only adequately predict the crack growth rate under variable amplitude loading. The Willenborg model has the advantage of not requiring an adjustable empirical constant but the Wheeler model can be better fitted to the experimental data if m is properly selected (69).

These two models only predict the delay following an overload and do not predict the acceleration following an underload nor do they predict the effect of multiple overloads. Some authors (70-72) have added correction factors to the Willenborg model to allow such predictions.

Gallagher and Hughes (70) introduced a proportionality factor, ϕ, which multiplies the second term of equations 31 and 32:

$$\phi = \frac{1 - \left[K_{TH}/K_{max,i}\right]}{B - 1} \qquad (33)$$

where K_{TH} is the threshold stress intensity factor for R=0 and B is the overload shut-off ratio ($K_{max,o}/K_{max,i}$) which produces no fatigue growth (73). This factor B in equation 33 takes into account the fact that some materials are more sensitive than others to overloads.

This model called the Generalized Willenborg Retardation Model has been used by Rudd and Engle (74) to predict the results of the ASTM round-robin investigation (25) previously mentioned. They obtained overly optimistic predictions which could be attributed to the fact they correctly took into account the delay caused by the overloads but not its cancellation caused by the underloads. However, the mean value of the ratio between the predicted life and the experiment is less than 2 which is still acceptable.

Johnson et al. (75,76) used a similar but more complex model called the Multi Parameter Yield Zone (MPYZ) model. In this model, equation 33 becomes:

$$\phi = \frac{1 - (K_{TH}/K_{max,i})}{(B/A-1) \times (1.0-R_L)} \qquad (34)$$

where A is the overload no-retardation ratio ($K_{max,o}/K_{max,i}$) below which no retardation takes place and $R_L = S_{UL}/S_{max,o}$ is the ratio of the largest underload following the overload S_{UL}, and the overload itself, $S_{max,o}$. Moreover, in their model, the plastic zone radius, r_{po}, is replaced by its diameter, Z_{OL}, in equations 31 and 32.

The effect of multiple overloads is taken into account by replacing B by B' in fquation 34 (77):

$$B' = \left[\frac{B - 2.0}{N_{OL}} \right] + 2.0 \qquad (35)$$

where N_{OL} is the number of successive overloads. When the plastic zone of the current cycle, Z_{op}, extends over the overload plastic zone, values of $K_{max,o}$, Z_{OL}, a_o and $S_{max,o}$ are replaced by those of $K_{max,i}$, Z_{ap}, a_i and $S_{max,o}$. For the overload cycle, it can be seen that the second term of equations 31 and 32 is negative and that acceleration occurs. In this case, equation 33 becomes:

$$\phi = \phi_A = (1 - R_L) \qquad (36)$$

and the amount of acceleration is adjusted to the ratio of the current underload. Finally, if the first part of the second term of equations 31 and

32 is noted

$$K_{eff,o} = K_{max,o} \left[\frac{1 - \Delta a}{Z_{OL}} \right]^{\frac{1}{2}} \qquad (37)$$

Johnson (76) suggests to replace it by

$$K'_{eff,o} = \left(\frac{K_{eff,o}}{Z-Y} \right) (Z-\beta) + K_{max} \qquad (38)$$

$$\text{where} \qquad \beta = \frac{K_{pr} - K_{UL}}{K_{eff,o} - K_{UL}} \qquad (39)$$

K_{pr} is the minimum value of the stress intensity factor in the i^{th} cycle preceding the overload, Y is the value of β under which the underload has no effect, and Z is the value of β for which the underload completely cancels the overload effect.

With the incorporation of all these factors, the predictions of Johnson (76) were better than those of Rudd and Engle (74) when applied to the same loading histories.

Chang et al. (78) also used the Generalized Willenborg Model (73) combined with the Chang acceleration principle (72) which applies when

$$R_{eff} = K_{min,eff}/K_{max,eff} < 0.$$

This model which will not be described here produced results similar to those of Johnson.

For all these models making use of equations similar to 33, 34 and 38, the determination of the parameters, A, B, Y and Z is important. Overload tests similar to those of Alzos, Hillberry and their co-workers (57, 79-81) and those of Chang et al. (78,82) can be used for that purpose.

A comparison made by Rudd and Engle (74) of the predictions (44,23,74,76,78) on models for prediction of fatigue crack growth under flight simulation loading (25) is shown on Figure 6. It can be seen that the predictions made by Johnson (76) and Chang et al. (78) are the most accurate. The Newman's predictions, based on a stronger theoretical background are also excellent but exhibit broader dispersion. As mentioned before, Rudd and Engle (74) who neglected the underloads effects, obtained non-conservative results.

Finally, it can be seen that quite acceptable results are obtained with a very simple RMS model (23) and even with a linear accumulation model neglecting sequence effects. It appears that, in the loading histories used for the investigation, the delay effects caused by the overloads and the damaging effect of the underloads mutually cancel. Unfortunately, this suggests that these loading histories represent a poor screening test to evaluate the precision of the different prediction models.

CONCLUSIONS

In many situations such as short block histories and stationary random loading, adequate predictions have been obtained with simple single parameter methods (RMS and RMN) since the overload effects are negligible. One important practical situation where the overload and underload effects are important is for flight simulation loading where the underload of the GAG cycle is particularly damaging. Complex cycle-by-cycle methods have proved to be more adequate for that particular situation.

Among the various cycle-by-cycle models the empirical ones have been preferred, for engineering purpose, to those based on stronger theoretical background. Even if the empirical models make use of some constants which have to be experimentally determined they are considered more reliable. However, on a longer term basis, it can be expected that the studies on the theoretical models will provide a better comprehension of the phenomenon and contribute to the development of simpler and more accurate models based on the fundamental material properties.

Most of the comparisons between the different models have been made with predetermined loading histories (fixed succession of peaks and valleys) based on a given service record or a simulation from a spectrum. However, a prediction based on the service record of a given individual structure (plane, car, offshore structure) might be very accurate for that particular record but not for an other record from a similar structure.

In fact, the available methods can now be considered to be more accurate than the accuracy with which the expected loading is known. The uncertainty in the loading comes from the fact that even similar structures in similar environments are submitted to slightly different loading histories. At the design stage, no service record is available and the prediction is based only on past experience with structures of the same type. Consequently, when the expected loading is known with very little accuracy, it is not justified to use very complex and accurate methods since most of the error will come from the lack of precise knowledge of the loading history itself.

REFERENCES

1. Paris, P.C., Gomez, M.P. and Anderson, W.E., The Trend in Engineering, 9-14 (1961).

2. Palmgren, A., Z. Vereines Deutscher Ingenieure, 68, 14, 339 (1924).

3. Miner, M.A., Trans. ASME, J. Appl. Mech., 67, A159 (Sept. 1945).

4. Nelson, D.V., Exp. Mech., 41-49 (Feb. 1977).

5. Schijve, J., Fatigue Crack Growth Under Spectrum Loads, ASTM STP 595, 3-23 (1976).

6. Lindley, T.C., in "La fatigue des matériaux et des structures", Maloine S.A., Paris, 341-410 (1980).

7. Dowling, N.E., J. of Mat., JMLSA, 7, 1, 78-87 (March 1972).

8. Dowling N.E., J. Test. Eval., 1, 4, 271-287 (July 1973).

9. Matsuishi, M. and Endo, T., Kyushu district meeting, Japan Society of Mechanical Engineers (1968).

10. Neuber, H., Trans. ASME, J. Appl. Mech., 83, 544-550 (1961).

11. Topper, T.H. Wetzel, R.M. and Morrow, J.D., J. Mat., 4, 1, 200-209 (March 1969).

12. Socie, D.F., Exp. Mech., 50-56 (Feb. 1977)

13. Elber, W., Eng. Fract. Mech., 2, 1, 37-45 (July 1970).

14. Elber, W., in Damage Tolerance in Aircraft Structures, ASTM STP 486, 230-242 (1971).

15. Stouffer, D.C. and Williams, J.F., Eng. Fract. Mech., 11, 3, 525-536 (1979).

16. Lanteigne, J. and Bailon, J.P., Met. Trans. A, 12A, 459-466. (March 1981)

17. Majumdar, S. and Morrow, J.D., in Fracture Toughness and Slow-Stable Cracking, ASTM STP 559, 159-182 (1974).

18. Kaisand, L.R. and Mowbray, D.F., J. Test. Eval., 7, 5, 270-280 (Sept. 1979).

19. Glinka, G., Robin, C. and Pluvinage, G., 9th Can. Fract. Conf., CFC9, (June 1983) to be publ. in Can. Met. Quat.

20. Barsom, J.M., in Progress in Flaw Growth and Fracture Toughness Testing, ASTM STP 536, 147-167 (1973).

21. Barsom, J.M., in Fatigue Crack Growth Under Spectrum Loads, ASTM STP 595, 217-235 (1976).

22. Sullivan, A.M. and Crooker, T.W., Trans. ASME, J. of Press. Vess. Techn., 98, 208-212 (Aug. 1976).

23. Hudson, C.M., in Methods and Models for Predicting Fatigue Crack Growth Under Random Loading, ASTM STP 748, 41-52 (1981).

24. Forman, R.G., Kearney, V.E. and Engle R.M., Trans. ASME, Journal of Basic Engineering, 89D, 3, 459-464 (1967).

25. Chang, J.B. and Hudson, C.M., ed. Methods and Models for Predicting Fatigue Crack Growth Under Random Loading, ASTM STP 748 (1981)

26. Paris, P.E., Proc. 10th Sagamore Army Materials Research Conference, 197 (1964).

27. Albrecht, P. and Yamada, K., in Service Fatigue Loads Monitoring, Simulation and Analysis, ASTM STP 671, 255-277 (1979).

28. Hibberd, R.D. and Dover, W.D., Fracture 1977, 2, ICF4, Waterloo, 1187-1194 (June 1977).

29. Dover, W.D., in Proc. Fracture Mechanics, Current Status, Future Prospects, Cambridge, 125-147, Pergamon (1979).

30. Dover, W.D., Int. J. Fat., 3, 2, 52-60 (April 1981).

31. Kitagawa, H., Fukuda, S. and Nishiyama, A., JSME Bulletin, 21, 153, 367-374 (March 1978).

32. Koterazawa, R., Materials, Experimentation and Design in Fatigue, Proc. of Fatigue 81, SEEFG Conference, Warwick University, (March 1981).

33. Buxbaum, O., in Service Fatigue Load Monitoring, Simulation and Analysis, ASTM STP 671, 5-20 (1979).

34. Lieurade, H.-P., in La fatigue des matériaux et des structures, Maloine S.A., Paris, 343-379 (1980).

35. Jeans, L.L. and Tribble, W.L., in Service Fatigue Loads Monitoring, Simulation and Analysis, ASTM STP 671, 246-254 (1979).

36. Pook, L.P. and Greenan, A.F., Int. J. Fat., 1, 1,17-22 (Jan. 1979).

37. Schijve, J., Report MP201, National Aeronautical Research Institute, Amsterdam (1961) presented to 2nd ICAF-AGARD Symposium Paris (May 1961).

38. Haibach, E. et al., Proc. Int. Conf. on Fatigue Testing and Design, Vol. 2, London, 29.1-29.21 (April 1976).

39. Schijve, J., Eng. Fract. Mech., 11 207-221 (1979).

40. Wirsching, P.J. and Light, M.C., ASCE J. Struct. Div., 106, 7, 1593-1607 (July 1980).

41. Elber, W., in Fatigue Crack Growth Under Spectrum Loads, ASTM STP 595, 236-250 (1976).

42. Socie, D.F., Eng. Fract. Mech., 9, 849-865 (1977).

43. Wetzel, R.M., ed., Fatigue Under Complex Loading: Analyses and Experiments, Advances in Engineering, 6, (1977).

44. Newman, J.C. Jr., Ref. 26, 53-84.

45. Newman, J.C., Jr., in Design of Fatigue and Fracture Resistant Structures, ASTM STP 761, 255-277 (1982).

46. Dugdale, D.S., J. of Mechanics and Physics of Solids, 8, 100-111 (1960).

47. DeKoning, A.U., in Fracture Mechanics: Thirteenth Conference ASTM STP 743, 63-85 (1981).

48. de Jonge, J.B. et al., NLR TR 73029U (March 1973).

49. Sunder, R., Eng. Fract. Mech., 12, 155-165 (1979).

50. Sunder, R., Eng. Fract. Mech., 12, 2, 147-154 (1979).

51. Lal, K.M., Garg, S.B.L. and Le May, I., J. Eng. Mat. Tech., 102, 147-152 (Jan. 1980).

52. Shiratori, M. et al., in Advances in Research on the Strength and Fracture of Materials, Fourth Int. Conf. on Fracture, Waterloo, 2B, 1091-1098 (1977).

53. Dill, H.D. and Saff, C.R., in Fatigue Crack Growth Under Spectrum Load, ASTM STP 595, 306-319 (1976).

54. Matsuoka, S. Tanaka, K. and Kawahara, M., Eng. Fract. Mech., 8, 3, 507-523 (1976).

55. Hardrath, H.F. et al., in Fracture Mechanics, University Press of Virginia, 347-364 (1978).

56. Buck, O., Frandsen, J.D. and Marcus, H.L., in Fatigue Crack Growth Under Spectrum Loads, ASTM STP 595, 101-112 (1976).

57. Alzos, W.X., Skat, A.C., Jr. and Hillberry, B.M., in Fatigue Crack Growth Under Spectrum Loads, ASTM STP 595, 41-60 (1976).

58. Von Euw, E.F.S., Hertzberg, R.J. and Roberts, R., in Stress Analysis and Growth of Cracks, ASTM STP 513, 230-259 (1972).

59. Shih, T.T. and Wei, R.P., Eng. Fract. Mech., 6, 19-32 (1974).

60. Suresh, S., Scripta Met., 16, 995-999 (1982).

61. Brown, R.D. and Weertman, J., Eng. Fract. Mech., 10, 867-878 (1978).

62. McMillan, J.C. and Pelloux, R.M.N., in Fatigue Crack Propagation, ASTM STP 415, 505-535 (1967).

63. Yokobori, Y., Konosu, S. and Yokobori, A.T., Jr., Fracture 77, 1, 665-82, Waterloo (June 1982).

64. McCartney, L.N., Int. J. Fract., 14, 2, 213-232 (April 1978).

65. Bernard, P.S., Lindley, T.C. and Richards, C.E., in Fatigue Crack Growth Under Spectrum Loads, ASTM STP 595, 78-79 (1976).

66. Willenborg, S., Engle, R.M. and Wood, H.A., AFFDL-TM-71-1-FBR (Jan. 1971).

67. Wheeler, O.E., Trans. ASME, J. Basic Eng., 94, 181 (1972).

68. Broek, D. and Smith, S.H., Eng. Fract. Mech., 11, 123-141 (1979).

69. Broek, D., Elementary Engineering Fracture Mechanics, Noordhoff International Publishing, Leyden, Netherlands, 408 (1974)

70. Gallagher, J.P. and Hughes, T.F., AFFDL-TR-74-27 (July 1974).

71. Johnson, W.S., NSRDC Report 4577 (Jan. 1975).

72. Chang. J.B., Engle, R.M. and Stolpestad, J., in Fracture Mechanics: Thirteenth Conference, ASTM STP 743, 3-27 (1981).

73. Gallagher, J.P., AFFDL-TM-FBR-74-28 (Jan. 1974).

74. Rudd, J.L. and Engle, R.M., Jr., Ref. 25, 103-114.

75. Johnson, W.S., Rister, W.C. and Spanner, T., J. Eng. Mat. Tech., ASME Trans., 100, 1, 57-63 (Jan. 1978).

76. Johnson, W.S., Ref. 25, 85-102.

77. Trebules, V.W., Roberts, R. and Hertzberg, R.W., in Progress in Flaw Growth and Fracture Toughness Testing, ASTM STP 536, 115-146 (1973).

78. Chang, J.B., Szamossi, M. and Liu, K.W., Ref. 25, 115-132.

79. Himmelein, M.K. and Hillberry, B.M., in Mechanics of Crack Growth, ASTM STP 590, 321-330 (1976).

80. Probst, E.P. and Hillberry, B.M., AIAA Journal, 12, 3, 330-335 (March 1974).

81. Hillberry, B.M., Skat, A.C., Jr. and Alzos, W.X., Proc. Int. Conf. on Fatigue Testing and Design, 2, London, 32.1-32.19, (April 1976).

82. Chang, J.B. and Stolpestad, J.H., ASSDL-TR-79-3036, Vol. 1, Air Force Flight Dynamics Laboratory (March 1978)

FIGURES

1. Schematic representation of the stress-strain response showing the closed hysterisis loops.
2. Typical strain-life curve showing the linear elastic and plastic strain-life relationship.
3. Samples of two stationary random signals with the same cumulative distribution of level crossings: a) Narrow-band signal with irregularity factor, I=.99; b) Wide-band signal with irregularity factor, I=.3 (from Haibach et al. (38)).
4. Illustration of the bar elements used by Newman (44) to model the behaviour of the plastic material at the crack tip and along the crack faces.
5. Wheeler model (67): a) plastic zone of the current cycle, r_{pi}, inside the overload plastic zone, r_{po}; b) Extension of the overload plastic zone, $a_o + r_{po}$ due to a new overload (from Broek (69)).
6. Comparison of the predictions submitted for the ASTM round-robin investigation on prediction models for fatigue crack growth under flight simulation loading (25) (from Rudd and Engle (74)).

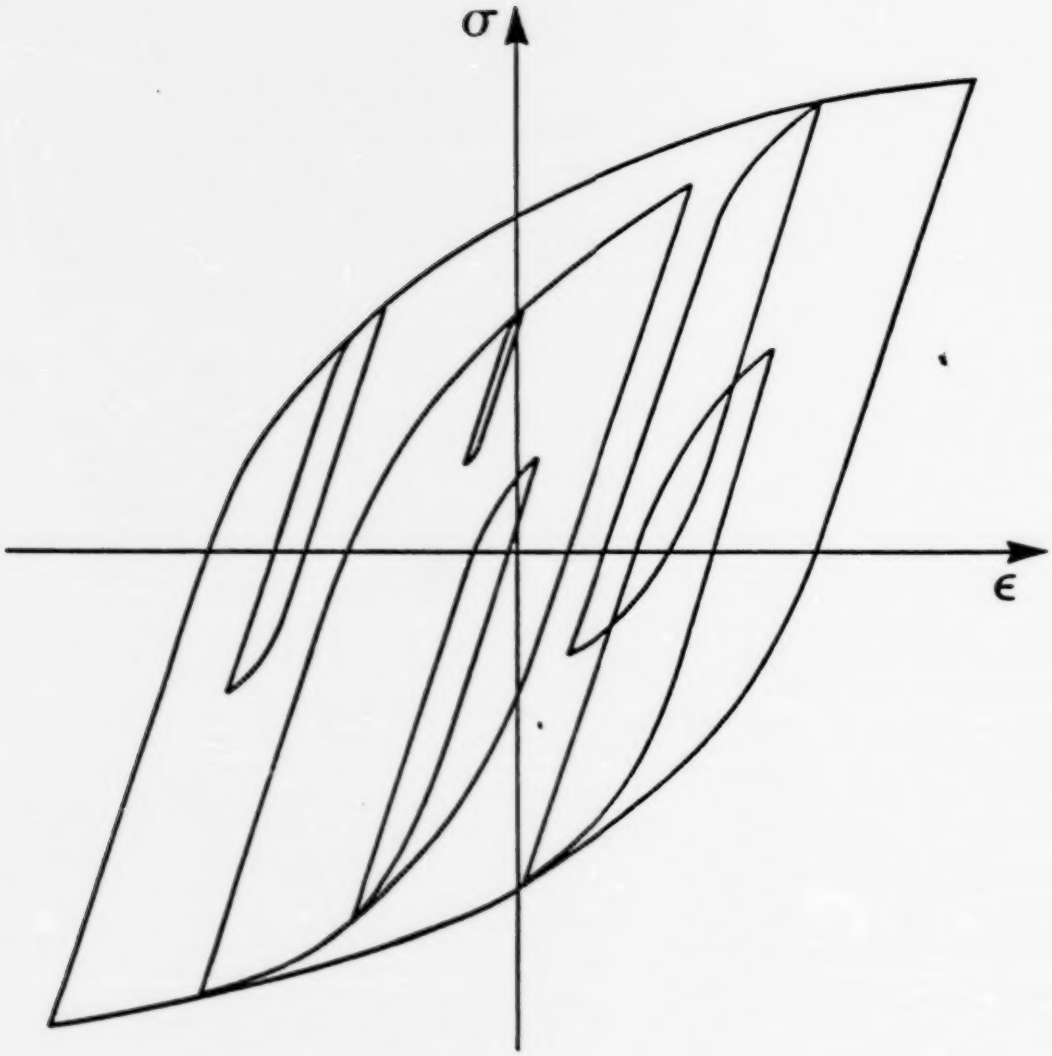

1. Schematic representation of the stress-strain response showing the closed hysterisis loops.

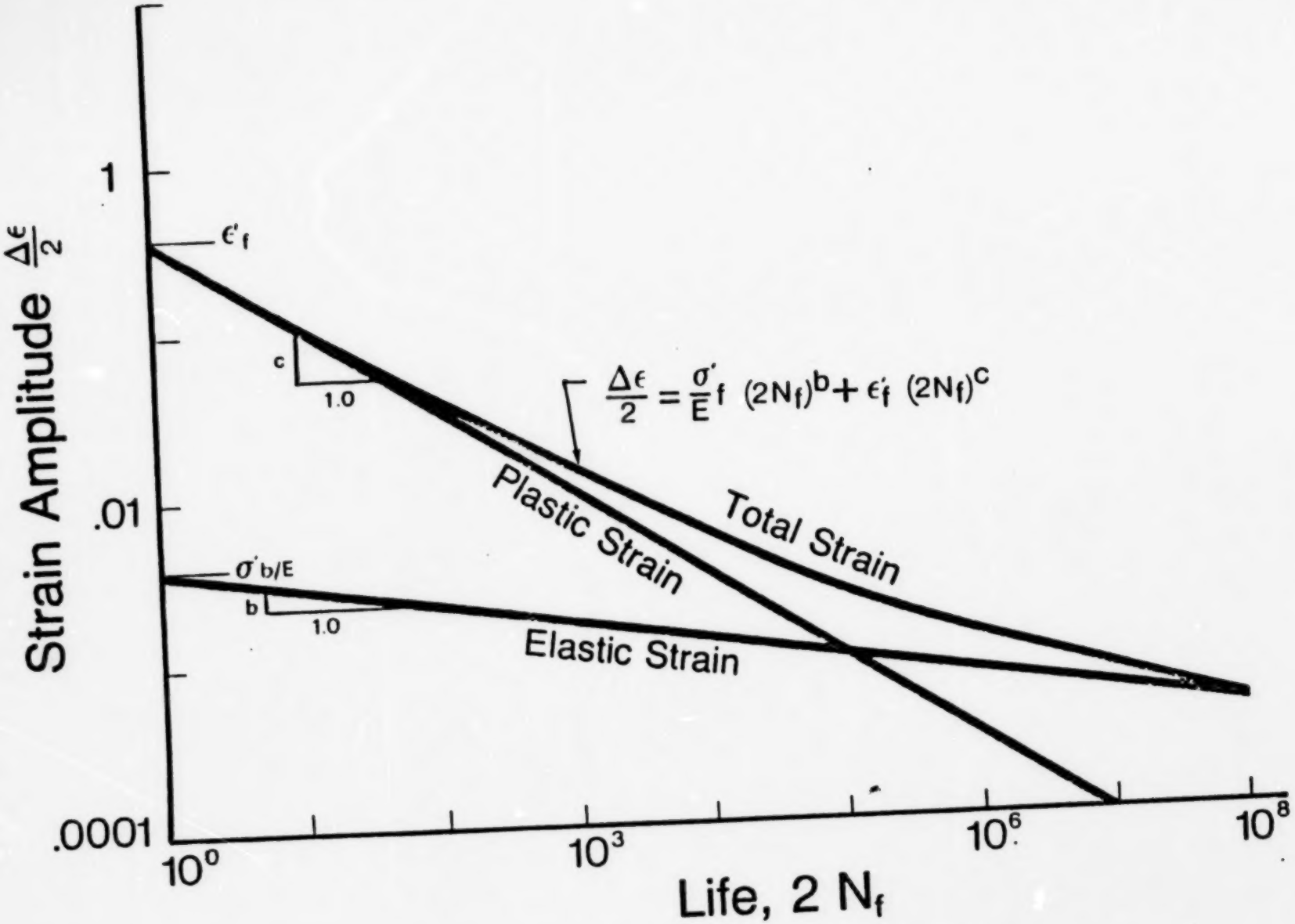

2. Typical strain-life curve showing the linear elastic and plastic strain-life relationship.

a)

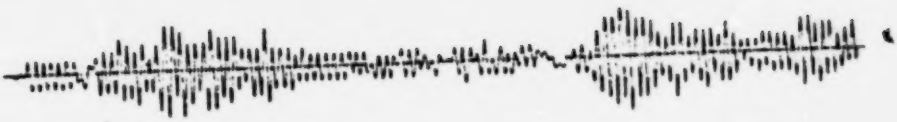

I = .99

b)

I = .3

3. Samples of two stationary random signals with the same cumulative distribution of level crossings: a) Narrow-band signal with irregularity factor, I=.99; b) Wide-band signal with irregularity factor, I=.3 (from Haibach et al. (38)).

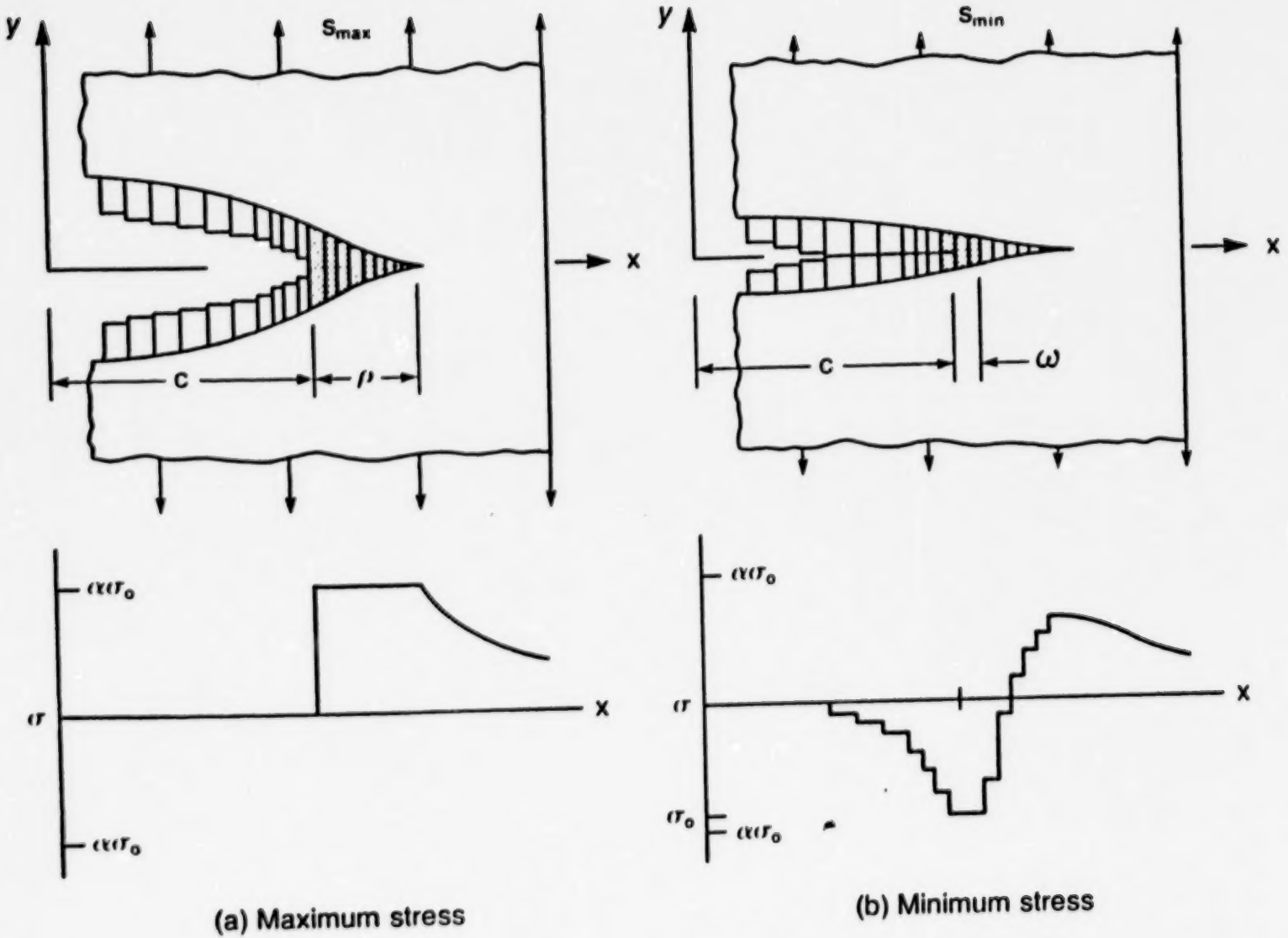

4. Illustration of the bar elements used by Newman (44) to model the behaviour of the plastic material at the crack tip and along the crack faces.

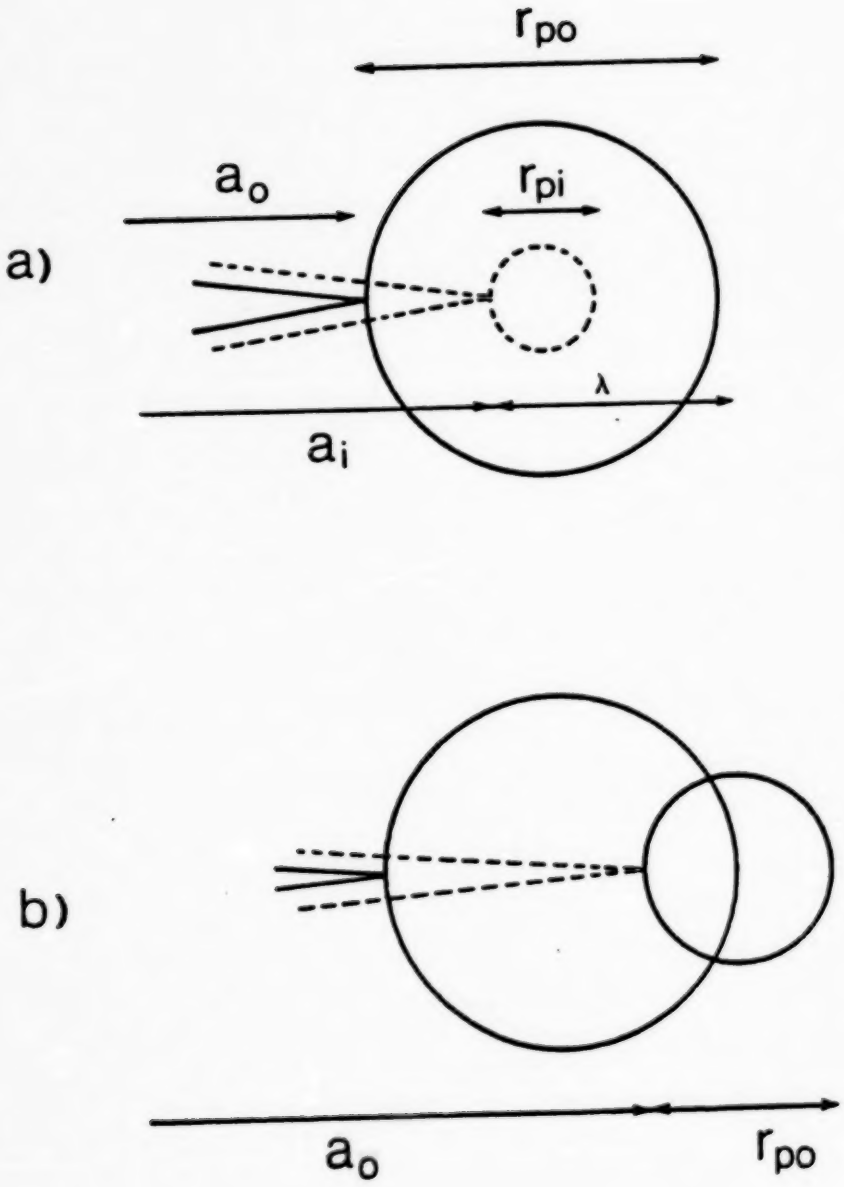

5. Wheeler model (67): a) plastic zone of the current cycle, r_{pi}, inside the overload plastic zone, r_{po}; b) Extension of the overload plastic zone, $a_o + r_{po}$ due to a new overload (from Broek (69)).

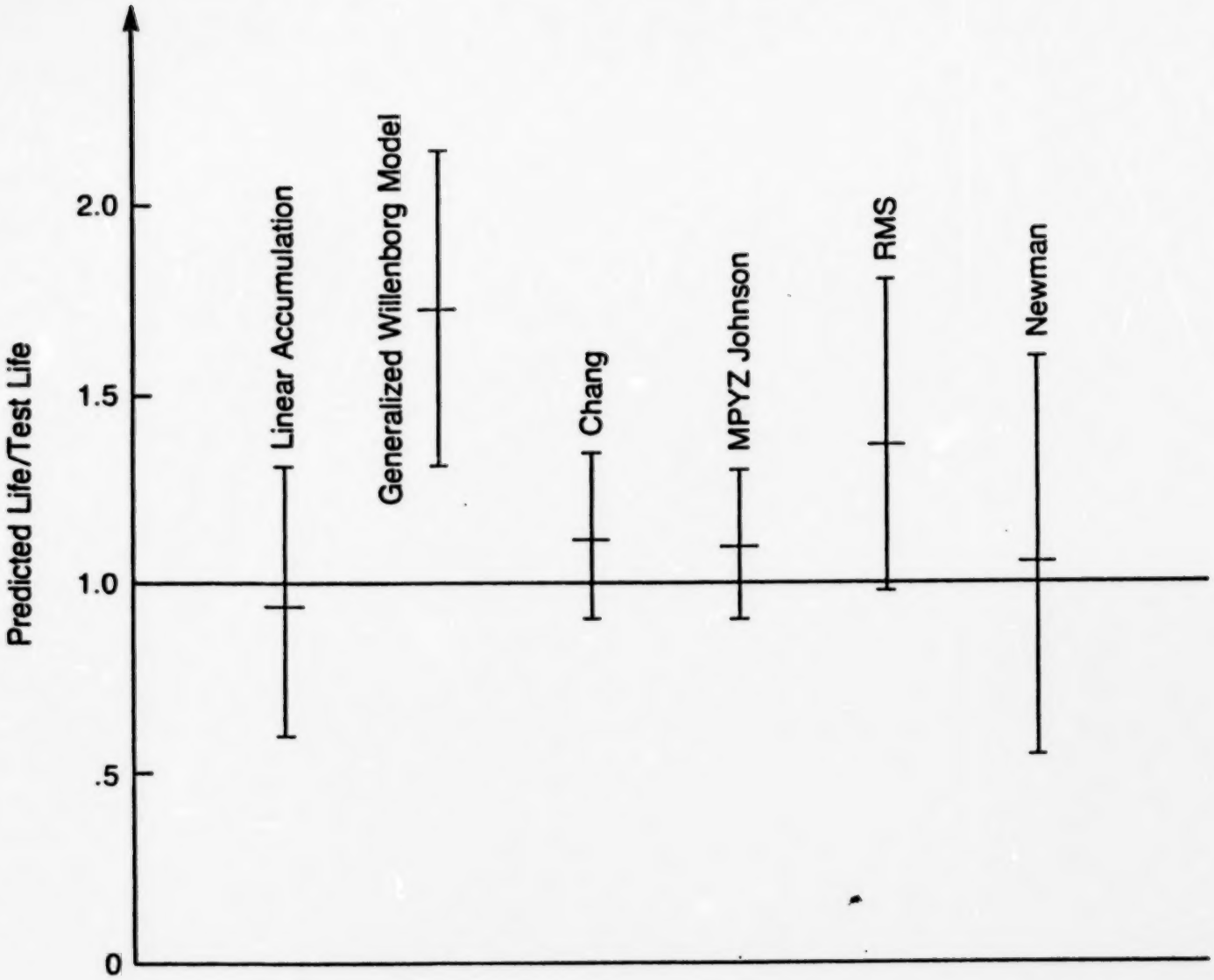

6. Comparison of the predictions submitted for the ASTM round-robin investigation on prediction models for fatigue crack growth under flight simulation loading (25) (from Rudd and Engle (74)).